Matter

CellPress

Article

Intrinsically cryopreservable, bacteriostatic, durable glycerohydrogel inks for 3D bioprinting

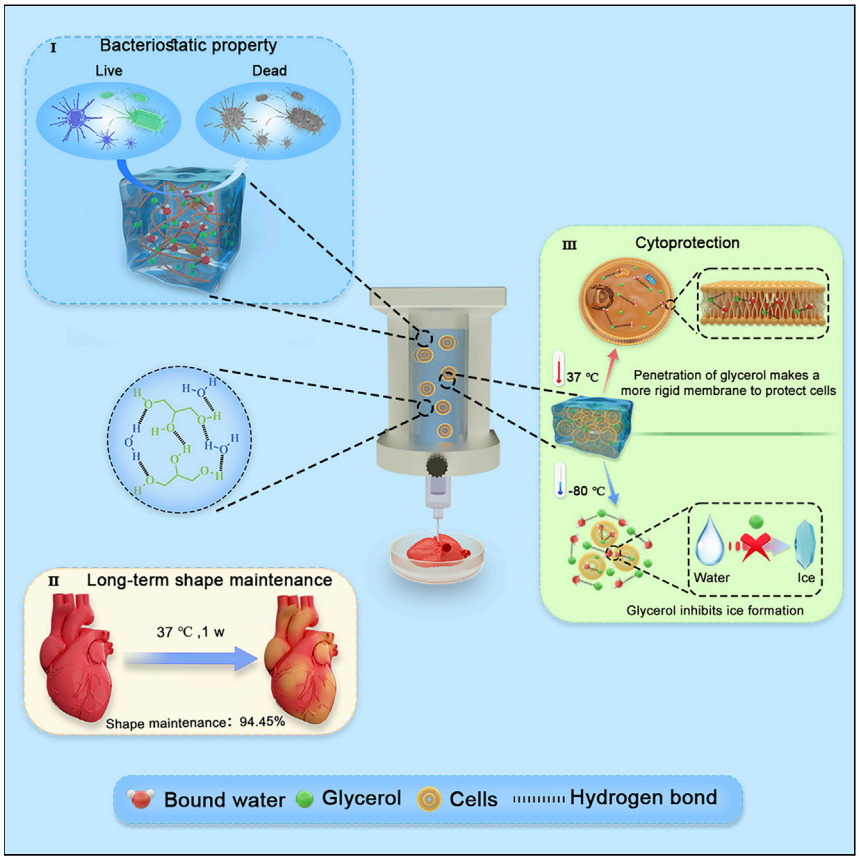

Liu et al. develop a glycerohydrogel bioink with excellent bacteriostatic properties, long-term shape maintenance, and cytoprotection ability. These features are highly desired but hard to achieve in existing bioinks. The key is using glycerol to regulate the water state in the bioink, resulting in limited "free water." This study sets up a paradigm of bioinks via molecular interactions and is expected to inspire a number of materials to facilitate practical utilization of 3D bioprinting.

Minglu Liu, Sihan Jiang, Nevin Witman, Huijing Wang, Wei Wang, Wei Fu, Zhengwei You

wangwei@scmc.com.cn (W.W.)
fuweizhulu@163.com (W.F.)
zyou@dhu.edu.cn (Z.Y.)

Highlights

A multifunctional binary glycerohydrogel bioink by regulating water state

High antimicrobial properties of glycerohydrogel bioinks against *E. coli* and mold

The shape maintenance of the glycerohydrogel bioinks is the longest ever recorded

Developed a cryopreservable bioink and provided a basis for future applications

Development
Practical, real world, technological considerations and constraints

Liu et al., Matter 6, 1–17
March 1, 2023 © 2023 Elsevier Inc.
https://doi.org/10.1016/j.matt.2022.12.013

Please cite this article in press as: Liu et al., Intrinsically cryopreservable, bacteriostatic, durable glycerohydrogel inks for 3D bioprinting, Matter (2023), https://doi.org/10.1016/j.matt.2022.12.013

Matter

CellPress

Article

Intrinsically cryopreservable, bacteriostatic, durable glycerohydrogel inks for 3D bioprinting

Minglu Liu,[1,5] Sihan Jiang,[2,5] Nevin Witman,[3] Huijing Wang,[4] Wei Wang,[1,*] Wei Fu,[4,*] and Zhengwei You[2,6,*]

SUMMARY

Three-dimensional (3D) printing of "bioinks" containing living cells has broad prospects in the fields of *in vitro* modeling and regenerative medicine. However, existing bioinks lack a number of required properties, including antibacterial characteristics, long-term shape maintenance, and cytoprotection ability during fabrication, cryopreservation, and transportation of 3D bioprinted tissues. In this study, we created a multifunctional glycerohydrogel bioink to address these challenges. The key is using glycerol to regulate the state of water in the bioink. Glycerohydrogels with limited "free water" exhibited significant inhibition of *Escherichia coli* and mold, outstanding shape maintenance, excellent compatibility with 3T3 mouse fibroblasts and rat adipose-derived stem cells, and an intrinsic ability of cryopreservation at −80°C, which is superior to existing hydrogel-based bioinks. This work provides a design principle for bioinks by regulating molecular interactions and will have broad prospects for practical biomedical applications.

INTRODUCTION

Three-dimensional (3D) bioprinting has gained increasing potential in biomedical applications in recent years because this technology makes it possible to prepare 3D tissue models of various morphologies with multiple cellular components for regenerative medicine and disease modeling.[1–5] Bioink is a key element in 3D bioprinting.[6,7] Hydrogels are currently the most commonly used bioinks because of their biomimetic extracellular matrix (ECM) properties.[8,9] Previous studies employing hydrogel bioinks have mainly focused on their cytocompatibility and cell survival after 3D bioprinting of tissues.[10–12] Formation of fatal ice crystals at low temperature makes cryopreservation of the resultant constructs challenging. Some researchers have reported anti-freezing hydrogels for bioelectronics and soft robots.[13] Recently, these types of hydrogels have also been investigated in biomedicine.[14,15] Luo et al.[16] pioneered this field; the team is known for elegant work in which they subjected cryo-bioprinting technology to temperatures between −5°C and −30°C using dimethyl sulfoxide- and melezitose-based bioink. Later, they further optimized the cryoprotective bioink, which could keep cell viability at −80°C and −196°C.[17] Because of its certain cytotoxicity, dimethyl sulfoxide is used in cryopreservation and needs to be removed at the cell culture stage. Furthermore, the widely used hydrogel bioinks provide a moist and closed environment for bacterial growth and suffer from water evaporation.[18,19] Overall, despite significant progress, the following challenges for 3D bioprinting remain: (1) suitable bacteriostatic characteristics of bioink,[20–22] (2) long-term shape maintenance of constructs,[23] and (3) cryopreservation of 3D-printed tissues.[13,16,24] Accordingly, an advanced bioink system is highly desired for practical applications in bioprinting.

PROGRESS AND POTENTIAL

3D bioprinting has increasing potential for biomedical applications. Hydrogels are currently the most commonly used bioinks. However, their practical application has been hampered by challenges such as ease of contamination, difficult cryopreservation, and poor long-term shape maintenance. Here, we propose a strategy of regulating the water state to create multifunctional glycerohydrogel bioinks with excellent bacteriostatic properties, long-term shape maintenance, and cytoprotection abilities superior to reported bioinks. This study sets up a paradigm of bioinks by regulating molecular interactions and is expected to inspire a number of materials to facilitate practical utilization of 3D bioprinting for a wide range of downstream applications, including *in vitro* modeling and regenerative medicine.

Water plays an important role in hydrogel bioinks and is critical for their properties. Water in hydrogels can be divided into three states: "free water," "weakly bound water," and "bound water."[25] Free water has almost no interaction with the polymeric network of hydrogels and shows thermodynamic behavior similar to that of ordinary pure water. The interaction between bound water and the hydrogel polymer network is strong.[26] Between free water and bound water, there is also some weakly bound water in the hydrogel. Generally, the free water in hydrogels can evaporate in ambient environments and freeze at low temperatures, providing an environment for bacteria to live, thus greatly limiting the practical application of hydrogel bioinks.[27] In view of this, we propose a bioink design principle that modulates the water state to endow it with favorable features.

Accordingly, a multifunctional binary glycerohydrogel bioink, in which glycerol was introduced to modulate the water state, was developed (Figure 1). The gel was based on a widely used biomacromolecule gelatin to ensure biocompatibility. The gelatin was crosslinked by glutaraldehyde via the Schiff reaction to form a relatively stable polymeric network (Figure 1A). The Schiff base contains dynamic imine bonds that enable crosslinking to reversibly dissociate under the force of 3D printing and reassociate after printing. This dynamic structural evolution endowed the resultant gel with shear-thinning and self-recovery properties to ensure its printability at room temperature. This feature overcomes the typical limitations of existing bioinks, which usually require harmful crosslinking reactions (e.g., UV light-induced radical addition[28,29]) after extrusion to ensure the structural integrity and mechanical properties of the resultant 3D-bioprinted constructs and achieve cell-friendliness throughout the 3D printing process. Moreover, this is the first example that aims to modulate the properties of bioink by regulating its "free water." Here, glycerol was introduced to the hydrogel to produce a binary glycerohydrogel as an advanced type of bioink. Glycerol forms extensive hydrogen bonds with water and polymeric networks, which reduces the content of "free water." Consequently, this significantly inhibits the growth of bacteria, volatilization, and freezing of the resultant bioink (Figure 1B). Accordingly, glycerohydrogel bioink is adaptable to a wide range of operating temperatures and environments.

In this study, we report the design, preparation, and characterization of binary glycerohydrogel bioink and demonstrate its bacteriostatic characteristics, excellent shape maintenance, cytoprotection during bioprinting, and cryopreservation of 3D-printed tissues, indicating its potential for clinical translation of biofabrication.

RESULTS AND DISCUSSION

Preparation and characterization of gelatin glycerohydrogels

Gelatin has been widely used as a bioink because of its excellent biocompatibility and low immunogenicity.[30] Because the physical gelation temperature of gelatin (30°C) is lower than the physiological temperature (37°C), gelatin must be modified to form a covalently crosslinked network to improve the stability of the gel.[30] Gelatin glycerohydrogels based on dynamic covalent imine crosslinks were prepared by introduction of glutaraldehyde, followed by solvent displacement. The Fourier transform infrared (FTIR) spectra showed that the intensity of the amide I band at approximately 1,630 cm^{-1}, arising from C=N stretching vibrations, significantly increased, confirming the formation of imine bonds between glutaraldehyde and gelatin (Figure 2A). In addition to the above changes, the enhanced intensity of the O-H stretching peak (3,280 cm^{-1}) indicated stronger hydrogen bonds among glycerol, water, and the polymeric network.[31]

[1]Department of Pediatric Cardiothoracic Surgery, Shanghai Children's Medical Center, School of Medicine, Shanghai Jiao Tong University, Shanghai 200127, China

[2]State Key Laboratory for Modification of Chemical Fibers and Polymer Materials, College of Materials Science and Engineering, Institute of Functional Materials, Donghua University, Research Base of Textile Materials for Flexible Electronics and Biomedical Applications (China Textile Engineering Society), Shanghai Engineering Research Center of Nano-Biomaterials and Regenerative Medicine, Shanghai 201620, China

[3]Department of Clinical Neuroscience, Karolinska Institutet, 17177 Stockholm, Sweden

[4]Institute of Pediatric Translational Medicine, Shanghai Children's Medical Center, School of Medicine, Shanghai Jiao Tong University, Shanghai 200127, China

[5]These authors contributed equally

[6]Lead contact

*Correspondence:
wangwei@scmc.com.cn (W.W.),
fuweizhulu@163.com (W.F.),
zyou@dhu.edu.cn (Z.Y.)

https://doi.org/10.1016/j.matt.2022.12.013

Please cite this article in press as: Liu et al., Intrinsically cryopreservable, bacteriostatic, durable glycerohydrogel inks for 3D bioprinting, Matter (2023), https://doi.org/10.1016/j.matt.2022.12.013

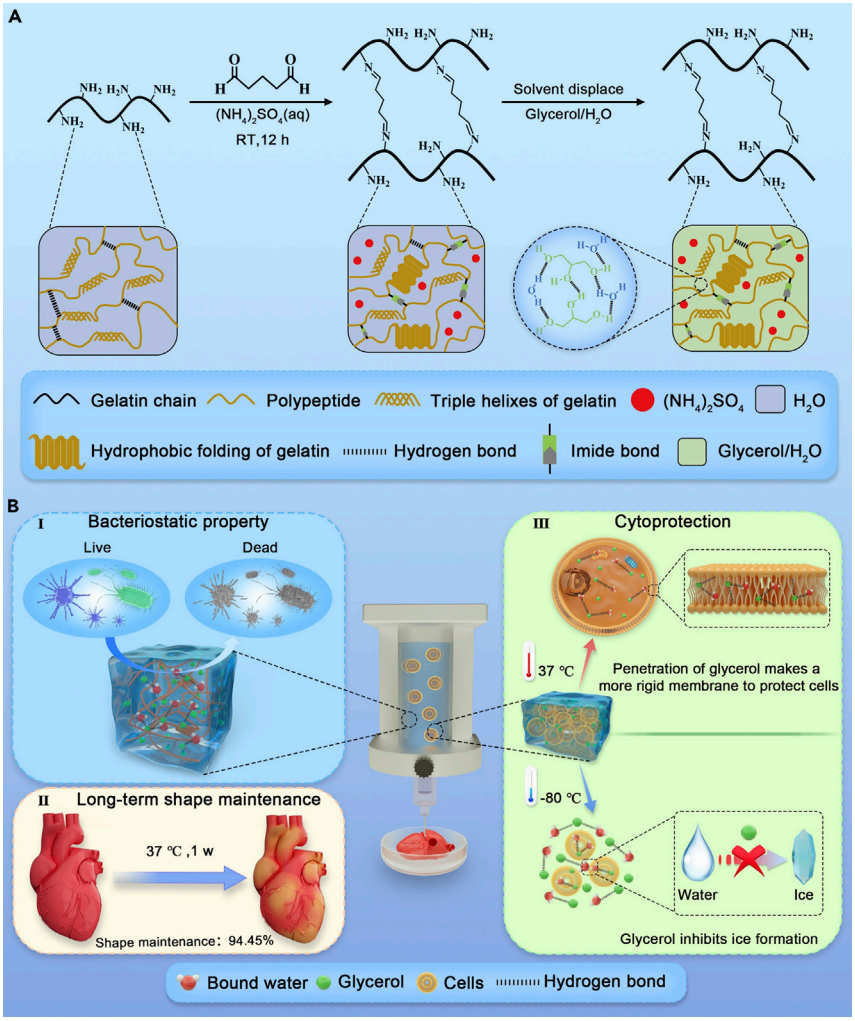

Figure 1. The development of multifunctional gelatin glycerohydrogel bioink

(A) Design and preparation of gelatin glycerohydrogel bioink.

(B) Three unique characteristics of gelatin glycerohydrogel bioink: bacteriostatic property (I), long-term shape maintenance (II), and cytoprotection during bioprinting and cryopreservation (III).

As an effective method to improve the thermal stability of gelatin, glutaraldehyde has been demonstrated to be nontoxic and not released from the materials at low concentration (0.1–1.5 wt %), which was attributed to formation of dynamic imine bonds.[32] To optimize the crosslinking formula, a stability test of glycerohydrogels with different crosslink densities was performed in a water bath (37°C). As shown in Figure S1, glycerohydrogels with a low degree of crosslinking ($NG_{0.2}T$; Table S1) were partially hydrolyzed after soaking for 12 h and completely disappeared after 24 h. For comparison, $NG_{0.6}T$ (with a medium degree of crosslinking) and NG_1T (with a high degree of crosslinking) gels maintained intact morphology after 7 days, indicating their stability at physiological temperature and in water medium. In view of the potential restriction of the high crosslinking degree on the dynamic of covalent networks, which was not conducive for bioprinting, glycerohydrogels with a medium degree of crosslinking ($NG_{0.6}T$) were used for further study. The characteristic peak on the mass spectrum confirmed that there was no free glutaraldehyde in the glycerohydrogels, ensuring their good biocompatibility (Figure S2).

Please cite this article in press as: Liu et al., Intrinsically cryopreservable, bacteriostatic, durable glycerohydrogel inks for 3D bioprinting, Matter (2023), https://doi.org/10.1016/j.matt.2022.12.013

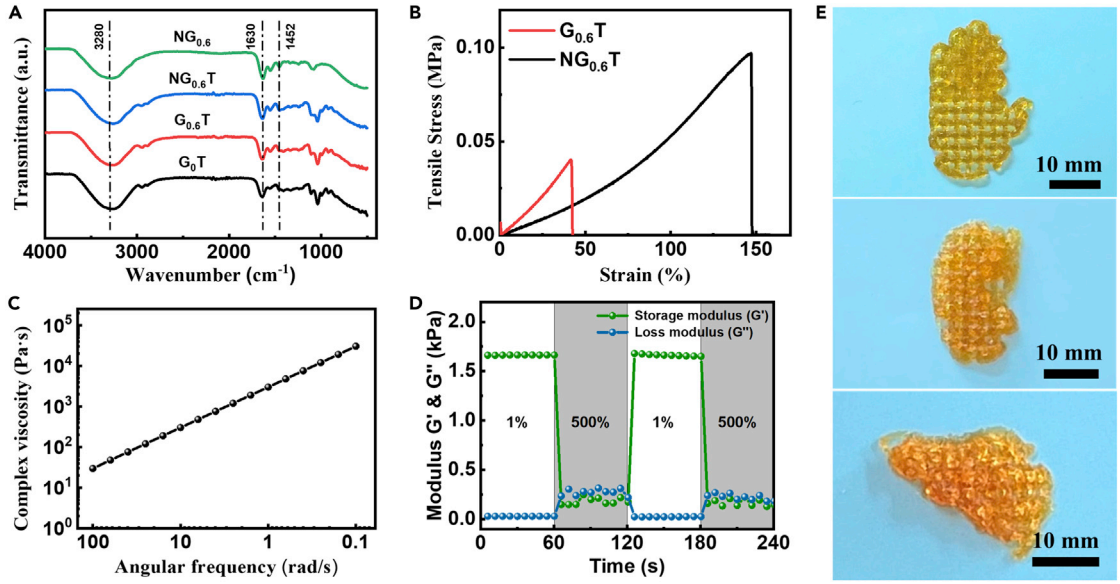

Figure 2. Characterization of gelatin glycerohydrogels

(A) FTIR spectroscopies of different gelatin hydrogels and glycerohydrogels.

(B) Tensile stress-strain curves of glycerohydrogels with different concentrations of $(NH_4)_2SO_4$.

(C) Viscosity of glycerohydrogels versus frequency by rheological test.

(D) Self-recovery through low (1% stain, 1 Hz) and high (gray part, 500% stain, 1 Hz) strain cycles of the rheological test.

(E) Images of 3D-printed glycerohydrogel constructs: hand, kidney, and liver shapes. Scale bars, 10 mm.

Bioinks made from gelatin usually suffer from poor mechanical properties that are not conducive to maintaining their shape post printing and limit their applications.[5,33] Ammonium sulfate has been reported to improve the mechanical properties of protein gels by enhancing hydrophobic interactions and chain entanglement.[34,35] Accordingly, we envisioned that ammonium sulfate could improve the mechanical properties of glycerohydrogels by inducing hydrophobic folding of gelatin molecular chains.[36] Compared with the glycerohydrogel without ammonium sulfate ($G_{0.6}T$), the tensile strength and maximum elongation of the glycerohydrogel ($NG_{0.6}T$) were improved by 2.3 times and 3.5 times, respectively, after soaking in aqueous glycerol solution mixed with $(NH_4)_2SO_4$ (Figure 2B; Table S2). The increased intensity of the C-H bending vibration and CH_3 symmetrical deformation vibration peak (1,452 cm^{-1}) shown in the FTIR spectra demonstrated the strong hydrophobic interactions formed by $(NH_4)_2SO_4$ (Figure 2A).[37]

In addition to stability and mechanical properties, for the extrusion-based printing process, shear-thinning characteristic during printing and rapid solidification after printing are two other crucial requirements for bioinks.[38] As a dynamic covalent bond, the imine bond can be dissociated reversibly under the shearing force of 3D printing, endowing glycerohydrogels with shear-thinning property to prevent cell damage due to extrusion pressure (Figure 2C). Furthermore, during rheological testing by applying alternating low and high strain, glycerohydrogels exhibited an excellent self-recovery property that rapidly transformed from gel-like behavior ($G' > G''$) at low strain (1%) to sol-like behavior ($G' < G''$) at high strain (500%) and quickly recovered after removing the strain (Figure 2D).[39] This property was also attributed to the dynamic nature of the crosslinked network, which met the need of quickly recovering to a gel state after extruding from the nozzle tip and overcame the limitation that most hydrogels require an additional crosslinking step after printing.[40,41] These two characteristics endowed glycerohydrogels with printability at

Please cite this article in press as: Liu et al., Intrinsically cryopreservable, bacteriostatic, durable glycerohydrogel inks for 3D bioprinting, Matter (2023), https://doi.org/10.1016/j.matt.2022.12.013

room temperature. The practical printability of glycerohydrogel was demonstrated by 3D printing of some graphic patterns (hand, kidney, and liver shapes) (Figure 2E).

Because free water accounts for the majority of hydrogels, its inevitable evaporation under ambient conditions has a detrimental effect on the performance of the hydrogel, including its mechanical properties, significantly hampering its use in a wide array of applications.[42,43] In contrast, glycerohydrogels were prepared by replacing a portion of free water with glycerol, exhibiting the excellent anti-drying property, and maintaining high stability because of the reduced content of water and the hydrogen bonds formed between glycerol, water, and the polymer network. The hydrogel and glycerohydrogel were simultaneously placed in a dry environment at 37°C to evaluate the anti-drying property. After 1 day of treatment, the original transparent hydrogel dried and became opaque (Figures S3AI, S3AII, S3BI, and S3BII). The modulus increased from 0.07 $\pm$ 0.01 MPa to 2.97 $\pm$ 0.84 MPa (Figure 3A), and the stress-strain curves of the cyclic tensile test of hydrogels exhibited an apparent change with a significant hysteresis (Figures 3B and S3C). Over time, loss of elasticity was evident among the hydrogels (Figures 3CI and 3CII). They became relatively brittle with a significantly reduced maximum elongation of less than 20% (Figure 3D), while the elastic modulus increased by more than 2,100 times after 3 days (Table S3). In contrast, the glycerohydrogels maintained high transparency and stretchability within 3 days (Figures 3CIII, 3CIV, S3AIII, S3AIV, S3BIII, and S3BIV), and the mechanical properties of the glycerohydrogels remained relatively stable (Table S4). The modulus remained unchanged for 3 days (0.06 $\pm$ 0.01 MPa), much smaller than the modulus of the hydrogel after 1 day (2.97 $\pm$ 0.84 MPa) (Figure 3A). The glycerohydrogel still exhibited a high maximum elongation of 194.57% $\pm$ 20.80% after 3 days (Figure 3D), significantly higher than that of hydrogels in the same period (16.93% $\pm$ 1.55%). Stress-strain curves of the cyclic tensile test of glycerohydrogels after 1 day at 37°C showed negligible hysteresis, almost consistent with the original recording (Figures 3E and S3D). Moreover, glycerohydrogels preserved elasticity on the third day (Figure S3E). These results revealed that glycerohydrogels were suitable candidate bioinks for long-term applications and showcased superior properties to hydrogels.

In addition to long-term stability, the remaining key challenge of hydrogel bioinks is their poor anti-freezing properties. Notably, water-based hydrogels are easily frozen at subzero temperatures because of the large amount of "free water" in the hydrogels, eventually leading to a brittle material.[7,44] Researchers have developed a range of strategies, including introduction of dimethyl sulfoxide,[17] inorganic salts,[13] ionic liquids,[45–47] and so on. Glycerol features excellent biocompatibility and forms extensive hydrogen bonds with water molecules, endowing glycerohydrogels with excellent anti-freezing property.[48] As shown in Figures 3F and S4, the hydrogel was frozen into a yellow solid at −80°C and lost its stretchability, whereas glycerohydrogels maintained elasticity after being stored at −80°C. Differential scanning calorimetry (DSC) was used to further evaluate the anti-freezing performance of the hydrogels and glycerohydrogels. As shown in Figure 3G, a sharp peak at approximately −22°C was observed on the curve, which was attributed to formation of ice crystals in the hydrogels. For glycerohydrogels, no crystallization peak was detected from −100°C to 20°C on the DSC thermogram, which indicated its excellent low-temperature tolerance. Moreover, hydrogels and glycerohydrogels were evaluated by non-destructive low-field nuclear magnetic resonance (LF-NMR) tests, reflecting the degree of freedom of water and distribution of water through evaluation of the spin-spin relaxation time (T_2; also known as transverse relaxation time). As shown in Figure 3H, the three peaks on the curve of each sample were linked to three states of water in the gel: bound water (corresponding to T_{21}, yellow area), weakly bound water (corresponding to T_{22}, orange area), and free

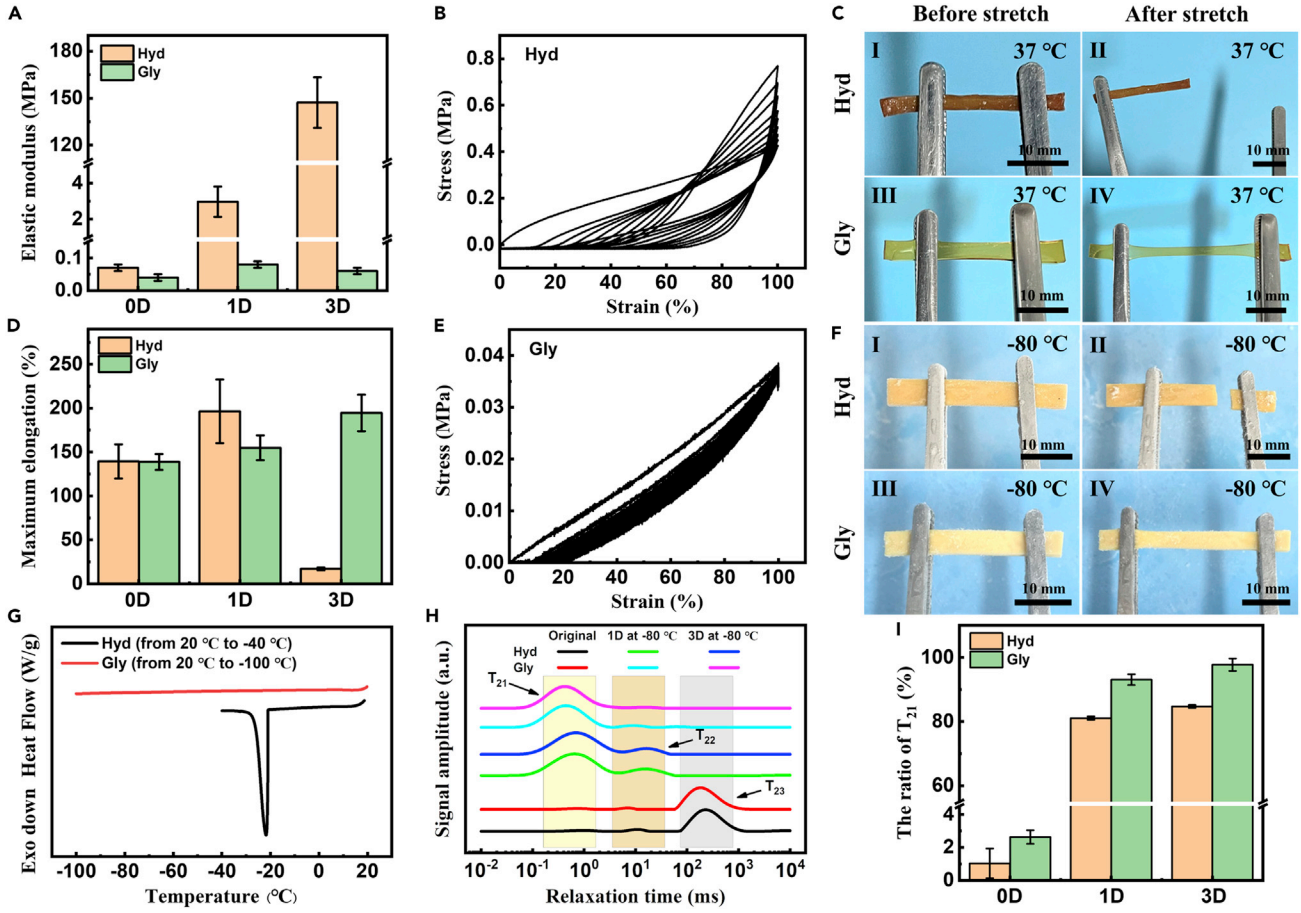

Figure 3. Anti-drying and anti-freezing properties of gelatin glycerohydrogels

(A) Elastic modulus of gelatin hydrogels (Hyd) and glycerohydrogels (Gly) stored at 37°C for different times.

(B) The cyclic tensile stress-strain curves of hydrogel stored at 37°C for 1 day with a strain of 100%.

(C) Photographs of Hyd (I and II) and Gly (III and IV) stored at 37°C for 3 days. The Hyd could not be stretched and was brittle at 37°C. Scale bars, 10 mm.

(D) Maximum elongation of Hyd and Gly stored at 37°C for different times.

(E) Cyclic tensile stress-strain curves of Gly stored at 37°C for 1 day with a strain of 100%.

(F) Photographs of Hyd (I and II) and Gly (III and IV) stored at −80°C for 3 days. The Gly maintained stretchability at −80°C. Scale bars, 10 mm.

(G) DSC thermogram of Hyd and Gly at a temperature change rate of 10°C/min

(H) Curves of spin-spin relaxation time (T_2) of Hyd and Gly stored at −80°C for different times.

(I) The effect of cryopreservation times on the ratio of bound water (T_{21}) of Hyd and Gly.

water (corresponding to T_{23}, gray area).[49] For glycerohydrogels, introduction of glycerol reduced the content of free water under normal conditions, shifted three peaks on the spectrum to a lower relaxation time, and demonstrated the content of bound water (97.73% ± 1.97%) (Table S5), which was higher than that of hydrogels stored at −80°C for the same time (84.73% ± 0.46%) (Figure 3I; Table S6). These phenomena were ascribed to the strong hydrogen bonds between glycerol and water molecules. These results demonstrated the excellent environmental adaptability and performance stability of glycerohydrogels, effectively expanding the application temperature range of the corresponding bioinks

Bacteriostatic properties of gelatin glycerohydrogel bioink

We next sought to evaluate the bacteriostatic properties of the glycerohydrogel because they are necessary to engineer functional biomaterials.[50] Live/Dead staining and bacterial growth curves of *Escherichia coli* (Gram negative) lasting 5 days on

Please cite this article in press as: Liu et al., Intrinsically cryopreservable, bacteriostatic, durable glycerohydrogel inks for 3D bioprinting, Matter (2023), https://doi.org/10.1016/j.matt.2022.12.013

glycerohydrogel patches were used to evaluate the bacteriostatic properties of the glycerohydrogel. Indeed, the glycerohydrogel group exhibited significant growth inhibition of *E. coli* based on Live/Dead bacteria imaging and bacterial growth curves compared with the gelatin hydrogel group (Figures 4A, 4B, S5A, and S5B). Scanning electron microscopy (SEM) of *E. coli* showed a smooth surface and intact cell membrane on gelatin hydrogels, whereas the glycerohydrogels showed a concave and rugate surface and distortion of the cell membrane (Figure 4C), which would induce leakage of the contents and destroy the physiological metabolism of *E. coli*.[51,52] Surprisingly, the glycerohydrogels exhibited similar significant growth inhibition of mold compared with the gelatin hydrogels (Figures 4D–4F and S5C).

The glycerohydrogels showed an apparent effect on bacterial growth inhibition. We concluded that the bacterium-inhibiting mechanism of glycerohydrogels occurred through monitoring of free water. The bacterium-inhibiting effect of glycerol can be explained by regulating the water state.[27,53] The presence of glycerol lowered the free water content of bacterial cells. Most organisms cannot cope with environments with low free water and either die or become dehydrated and dormant. Moreover, glycerol penetrates bacterial cells by facilitating diffusion and inhibiting the efflux of water from bacterial cells.[54] Osmotic pressure increases and causes weakening of the membrane and cellular lysis, depending on the resistance of the cell wall. This is the first study reported so far to add glycerol to hydrogels to inhibit bacterial growth.

Long-term medium free shape maintenance of the gelatin glycerohydrogel bioink scaffolds

Shape maintenance is one of the main aspects of bioink scaffolds that influence their functionality.[55] A specific shape is desired when a construct is printed. However, because hydrogels are mostly water, it is hard to achieve adequate shape maintenance upon deposition, and they typically need to be printed in a culture medium.[56] In contrast, gelatin glycerohydrogel retains glycerol after printing, so the bioink has excellent shape-maintenance capabilities without external culture medium. Moreover, medium-free printing is more convenient and less prone to contamination. To verify the shape-maintenance capabilities of the glycerohydrogels, we modeled the shape of the human heart and ear using gelatin glycerohydrogels and hydrogels (Figures 5A, 5B, S6A, and S6B). Following 3D printing, the glycerohydrogel scaffolds largely maintained the heart shape for the duration of *in vitro* culture, whereas the hydrogel scaffolds showed rapid shrinkage over time. The shape maintenance of engineered heart scaffolds was retained at 98.07% and 78.96% after 3 days and 21 days post printing, respectively (Figure 5B). This was a significantly better outcome compared with the hydrogel controls, whose shape similarity was only retained at 89.42% and 43.59% after 3 days and 3 weeks post printing, respectively (Figure 5A). The glycerohydrogels exhibited 1.93% shrinkage after drying at room temperature for 3 days and were sufficient to maintain the heart shape for 3 weeks. Moreover, the heart-shaped glycerohydrogel scaffolds revealed enhanced structural integrity of several characteristics, including weight, length, and width maintenance, compared with gelatin hydrogel scaffolds (Figures 5C–5E). The superiority of the glycerohydrogel-printed scaffolds to maintain structural shape retention over hydrogel-printed scaffolds was attributed to the hydrogen bonds formed between glycerol and water molecules, which inhibited the volatilization of water endowing the glycerohydrogel with excellent anti-drying properties.[48] Overall, the glycerohydrogel bioinks offered better long-term shape maintenance and endurance than the typical hydrogel bioink and, thus, were more suitable for biomedical applications under air conditions, such as hydrogel patches for wound healing and corneal repair.

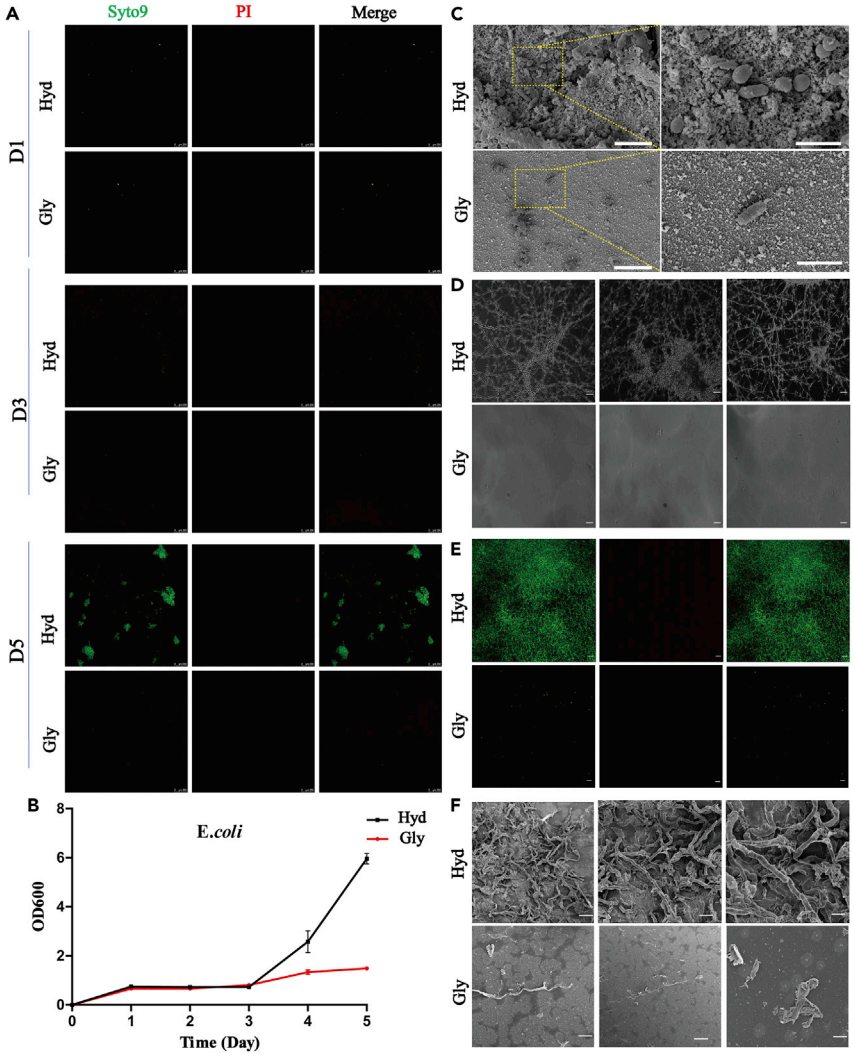

Figure 4. Antibacterial properties of gelatin Gly bioink

(A) Live/Dead assay of *E. coli* on days 1, 3, and 5 on the Gly group and hydrogel group. For each panel, the left image shows Syto9 staining (live bacteria), the center shows PI staining (dead bacteria), and the right shows superposition. Scale bars, 250 μm.

(B) Bacterial growth curves for *E. coli* on different days.

(C) The cell morphology and membrane damage of *E. coli* on Gly and Hyd on day 5 were observed by SEM Scale bars, 5 μm (left) and 2 μm (right).

(D) The growth of the molds in their natural environment was imaged using bright-field microscopy. Scale bars, 100 μm.

(E) Mold Live/Dead assay on Gly and Hyd. For each panel, the left image shows Syto9 staining (live fungus), the center shows propidium iodide (PI) staining (dead fungus), and the right shows superposition. Scale bars, 100 μm.

(F) The cell morphology and membrane damage of molds on Gly and Hyd were observed by SEM. Scale bars: 15 μm (left), 10 μm (medium), and 5 μm (right).

Cytoprotection during 3D bioprinting and cryopreservation of gelatin glycerohydrogel bioink

Biocompatibility is an essential feature of bioink. Therefore, we next sought to explore the biocompatibility of glycerohydrogel bioinks with different kinds of cells. We performed Live/Dead staining and Cell Counting Kit 8 (CCK-8) proliferation assays on two cell types: 3T3 mouse fibroblasts and rat adipose-derived stem cells

Please cite this article in press as: Liu et al., Intrinsically cryopreservable, bacteriostatic, durable glycerohydrogel inks for 3D bioprinting, Matter (2023), https://doi.org/10.1016/j.matt.2022.12.013

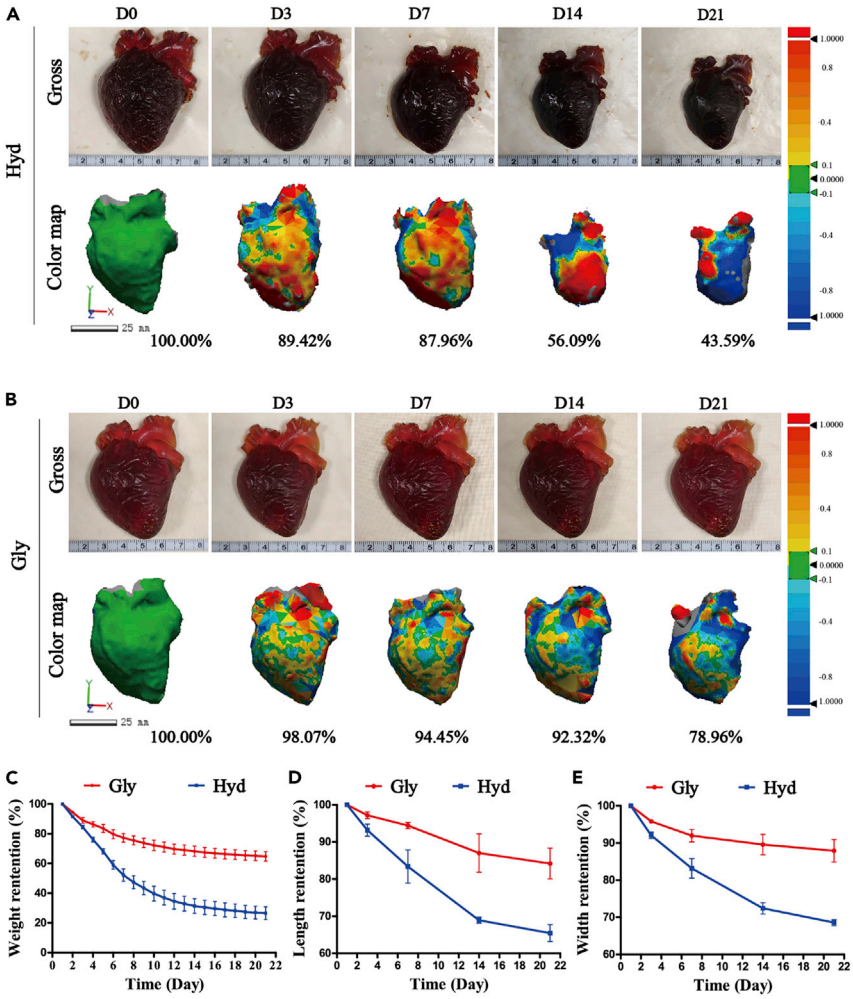

Figure 5. Shape maintenance of gelatin Gly bioink

(A and B) Physical map for the Hyd (A) and Gly (B) on days 0, 3, 7, 14, and 21.

(C) Weight retention curve over time of heart scaffolds made of Hyd or Gly.

(D) Length retention curve over time of heart scaffolds made of Hyd or Gly.

(E) Width retention curve over time of heart scaffolds made of Hyd or Gly.

(rADSCs). The cells embedded in glycerohydrogel patches revealed superior support of cell viability and proliferation over gelatin hydrogel controls (Figure S7). Cytoprotection is a key element of 3D bioprinting. Thereafter, we sought to prepare a 3D bioprinting ink of 3T3 cells and a gel mixture for a cell viability assay. After bioprinting for 3 days, the proportion of Calcein-AM 3T3 cells in glycerohydrogel bioink (65.48% $\pm$ 12.28%) was significantly higher than that in hydrogel bioinks (33.73% $\pm$ 12.37%, $p < 0.05$) (Figures 6A and 6E). Moreover, such 3D bioprinting did not require a culture medium, which is usually necessary when using a typical hydrogel bioink; therefore, it is more convenient and less prone to contamination. These results, combined with previous material characterization of glycerohydrogels (Figure 3), indicated that glycerol had a high binding ability to the water in glycerohydrogels and cells, which could transform the free water in the constructs into bound water, inhibiting water evaporation. Moreover, glycerol penetrates and alters the structural arrangement of phosphatidylcholines, a major lipidic component of the cell membrane.[57,58] The subsequent expansion of the lipid molecular area and changing

Please cite this article in press as: Liu et al., Intrinsically cryopreservable, bacteriostatic, durable glycerohydrogel inks for 3D bioprinting, Matter (2023), https://doi.org/10.1016/j.matt.2022.12.013

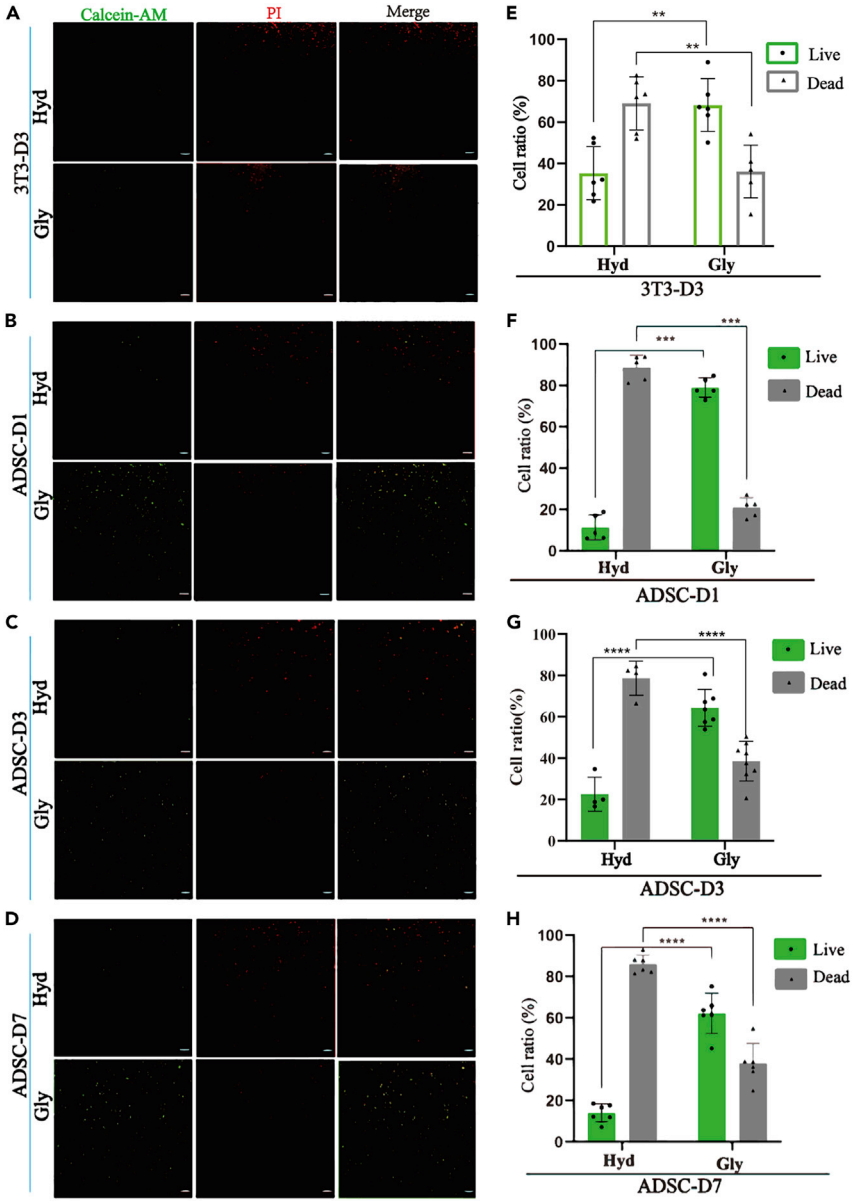

Figure 6. Viability of cells in gelatin Gly bioink during 3D bioprinting and following cryopreservation

(A) Live/Dead assay of 3T3 cell 3D bioprinting on day 3 on the hydrogel group and Gly group. For each panel, the left image shows Calcein-AM staining (live cells), the center shows PI staining (dead cells), and the right shows superposition. Scale bars, 100 μm.

(B–D) Live/Dead assay of cryopreserved ADSCs (−80°C) on day 1 (B), day 3 (C), and day 7 (D) on the Gly group and Hyd group. Scale bars, 100 μm.

(E) The statistical results of the Live/Dead of 3T3 cell percentage 3D bioprinting on day 3.

(F–H) The statistical results of the Live/Dead assay of cryopreserved ADSC percentage on day 1 (F), day 3 (G), and day 7 (H). Error bars represent SD; $n \geq 3$ for each group; ***$p < 0.001$ versus the control group.

the orientation of choline in the gel phase alter the bilayer structure. These changes constrain acyl chains and alter the lipid order, resulting in a more rigid structure (Figure 1). Glycerol can reduce the outflow of intracellular water molecules because of its hypotonic activity and improve cell survival.

Please cite this article in press as: Liu et al., Intrinsically cryopreservable, bacteriostatic, durable glycerohydrogel inks for 3D bioprinting, Matter (2023), https://doi.org/10.1016/j.matt.2022.12.013

Cryopreservation of 3D-printed tissues is vital for practical biomedical applications. We carried out the viability assay of ADSCs and 3T3 cells in glycerohydrogels as well as gelatin hydrogels to evaluate the effects of bioinks on cryopreserved cells at −80°C (Figures 6B–6D). As shown in Figures 6F–6H, post cryopreservation and recovery, the proportions of Calcein-AM ADSCs on days 1, 3, and 7 in glycerohydrogels were 79.05% ± 4.70%, 63.72% ± 8.94%, and 62.09% ± 9.74%, respectively. The proportions of Calcein-AM ADSCs on days 1, 3, and 7 in gelatin hydrogels were only 11.37% ± 6.09%, 21.94% ± 8.22%, and 13.99% ± 4.39%, respectively. The viability of cryopreserved cells in glycerohydrogels was significantly higher than that in the gelatin hydrogels ($p < 0.05$). Similar results were revealed in 3T3 cells (Figures S8A–S8G). Furthermore, we performed experiments to evaluate the effect of glycerol concentration on cryopreservation. On day 1, the proportions of Calcein-AM 3T3s in glycerohydrogels with 0%, 25%, 50%, and 75% glycerol were 7.06% ± 1.82%, 12.56% ± 4.14%, 55.67% ± 0.56%, and 68.46% ± 7.17%, respectively. The viability of cryopreserved cells in 75% glycerol glycerohydrogels was significantly higher than that in the 50% glycerol glycerohydrogels ($p < 0.05$) (Figures S9A–S9F). In addition, inks with different glycerol concentrations (0%, 25%, 50%, and 75%) and cryopreservation in liquid nitrogen (−196°C) were investigated (Figures S10 and S11). On day 1, the proportions of Calcein-AM 3T3s in gels with 0%, 25%, 50%, and 75% glycerol concentration were 11.59% ± 6.64%, 26.68% ± 3.03%, 46.07% ± 9.37%, and 62.51% ± 12.34%, respectively (Figure S10). The viability of cryopreserved cells in 75% glycerol glycerohydrogels in liquid nitrogen was significantly higher than that in 50% glycerol glycerohydrogels at −80°C ($p < 0.05$) (Figure S11). Furthermore, the viability of cryopreserved cells in 50% and 75% glycerol glycerohydrogels in liquid nitrogen is comparable with the one at −80°C. These results demonstrated that an increase in glycerol concentration could improve the cryopreservation effect. We could further improve its cryopreservability by optimizing the ink formulation in the future.

Based on the observations described above, we concluded that the glycerohydrogel bioink possessed the characteristics of cytoprotection during bioprinting and cryopreservation of 3D-printed tissues. The preceding cryopreservation results for the glycerohydrogel bioink could be influenced by dynamic changes in water.[59] Glycerol has been used as a permeable cryoprotectant to penetrate cellular membranes and provide intracellular cryoprotection;[60–62] they can localize around the polar head group of phospholipids via polar interactions and replace the localized water molecules to penetrate the cellular membrane. Glycerol can also bind water molecules via hydrogen bond interactions and inhibit intracellular and extracellular ice formation to prevent typical "two-factor cryoinjury" and improve the survival ability of cryopreserved cells.[63] This hypothesis was also evident by DSC results of glycerohydrogel and hydrogel (Figure 3G). Overall, the ice formation inhibition effect and 3D cell supporting ability of glycerohydrogel bioinks make them favorable for 3D bioprinting and cryopreservation.

Conclusions

Taking a design principle of regulating the state of water, we created a type of bioink, multifunctional binary glycerohydrogels. The glycerohydrogel bioink exhibited unprecedented features, including superior bacteriostatic characteristics, long-term shape maintenance, and intrinsic cryo-preservability of 3D-printed constructs, which are important for precise construction of multiple tissues, an inherent requirement and trend of 3D bioprinting. Especially the long-term cryopreservation ability endows glycerohydrogel bioinks with tremendous potential for future clinical translation of biofabrication and has been barely reported previously. In our follow-up study, we will optimize the formulation of bioinks, including the polymeric network

Please cite this article in press as: Liu et al., Intrinsically cryopreservable, bacteriostatic, durable glycerohydrogel inks for 3D bioprinting, Matter (2023), https://doi.org/10.1016/j.matt.2022.12.013

and liquid phases, to deliver better properties, especially cell survival ratio after cryo-preservation, and promote their application to construct real tissues. This work sets up a paradigm of bioinks and is expected to inspire a family of bioinks to facilitate practical utilization of 3D bioprinting for a wide range of fields, such as *in vitro* disease modeling and regenerative medicine.

EXPERIMENTAL PROCEDURES

Resource availability

Lead contact

Further information and requests for resources and reagents should be directed to and will be fulfilled by the lead contact, Zhengwei You (zyou@dhu.edu.cn).

Materials availability

This study did not generate new unique reagents.

Data and code availability

This study did not generate custom code, software, or algorithms. Additional data of this study are available from the corresponding authors upon reasonable request.

Materials

Gelatin (type A, from porcine skin, 300 Bloom) and glycerol (≥99.0%) were purchased from Sigma-Aldrich. $(NH_4)_2SO_4$ (≥99.5%) was purchased from Titan (Shanghai). Glutaraldehyde (50% in H_2O) was purchased from Macklin. $Ca(NO_3)_2 \cdot 4H_2O$ (≥99.0%) was provided from Sinopharm Chemical. Deionized water was used in the experiments. All reagents were used as received.

Fabrication of gelatin hydrogel and glycerohydrogel

Gelatin powder (30 g) and $Ca(NO_3)_2 \cdot 4H_2O$ (5 g) were dissolved in deionized water (100 g) and stirred at 50°C until clear and there were no bubbles. Subsequently, a certain amount of gelatin aqueous solution was squeezed into a watch glass, placed in the refrigerator for 30 min for gelation, and then put into a glutaraldehyde-containing ammonium sulfate aqueous solution at room temperature for 12 h to synthesize crosslinked gelatin hydrogel. After rinsing with water three times, the crosslinked gelatin hydrogels were soaked in a mixed solution made of ammonium sulfate aqueous solution (9.09 wt %) and glycerol at a mass ratio of 3:1, 1:1, and 1:3 for 12 h to prepare crosslinked gelatin glycerohydrogels. For comparison, the crosslinked gelatin hydrogel was fabricated using the same process using ammonium sulfate aqueous solution alone without glycerol.

For convenience of further discussion, we defined the gelatin hydrogels and glycerohydrogels (the mass fraction of glycerol in the mixed solution was 50%) as NG_x and NG_xT in short, respectively, where "N," "G," and "T" represent ammonium sulfate, glutaraldehyde, and glycerol respectively, and "x" represents the concentration of glutaraldehyde used in the crosslinking reaction. G_0T represents gelatin glycerohydrogels that were not crosslinked with glutaraldehyde. The formulas of the reaction solution for preparing crosslinked gelatin hydrogels are shown in Table S1.

Characterization and measurement

The chemical structures were measured by attenuated total reflection FTIR (ATR-FTIR) (Nicolet iS5, Thermo Fisher Scientific, USA) and gas chromatography-mass spectrometry (GCMS-QP2010Ultra, USA). LF-NMR was performed on a MesoMR23-060H-I analyzer (Niumag Electric, Shanghai, China). The transverse relaxation time was obtained by Carr-Purcell-Meiboom-Gill sequence (CPMG) with

Please cite this article in press as: Liu et al., Intrinsically cryopreservable, bacteriostatic, durable glycerohydrogel inks for 3D bioprinting, Matter (2023), https://doi.org/10.1016/j.matt.2022.12.013

90° and 180° pulses of 7.00 and 14.48 μs, respectively (echo time, 0.30 ms; echo numbers, 10,000; repetition time, 2,000 ms). Four repeat scans were performed. Finally, the CPMG data were converted by Multi-Exp Inv Analysis software to obtain the spin-spin relaxation time distribution. Tensile tests were performed on an MTS (Mechanical Testing & Simulation) machine equipped with a 100N loading cell at a deflection rate of 50 mm/min. At least three specimens were tested and averaged for each sample. In the cyclic tensile test, the specimens were elongated to a strain of 100% at deflection recovery rate of 20 mm/min for 10 cycles. DSC (204F1, Netzsch) was performed at a temperature change rate of 10°C/min under a nitrogen atmosphere. The stability of the glycerohydrogels with different crosslinking densities were evaluated in a 37°C water bath. Frequency sweep experiments of the glycerohydrogel were performed using a DHR-2 rheometer (TA Instruments, USA) at 25°C with a constant strain of 1% in the angular rate range of 100–0.1 rad/s. Self-recovery studies were performed using a DHR-2 rheometer (TA Instruments, USA) at 25°C with alternating low (1%) and high (500%) strains (1 Hz, 60 s) for two cycles.

Cell culture

Wistar rats (6 weeks old) were purchased from JSJ-LAB (Shanghai, China). The Animal Care and Experiment Committee of Shanghai Children's Medical Center approved the experimental protocols. ADSCs were isolated from the adipose tissue of both inguinal regions of rats; then, the adipose tissue was cut into pieces and treated with 0.1% (w/v) collagenase type II (NB4; Serva, Heidelberg, Germany) in serum-free low-glucose Dulbecco's modified Eagle's medium (DMEM; HyClone, USA) at 37°C for 1 h. The cells were concentrated and then seeded into tissue culture flasks in DMEM containing 10% fetal bovine serum. The cells were cultured to 80% confluence before passaging. ADSCs of passages 2–3 were used for the experiments. ADSCs were grown in mesenchymal stem cell (MSC) culture medium (Sciencell, USA) supplemented with 5% fetal bovine serum (FBS), 1% MSC growth supplement, 100 U/mL penicillin, 100 μg/mL streptomycin, and glutamine at 37°C in a humidified atmosphere consisting of 5% CO_2, and the medium was changed every 3 days. When cells reached 70%–80% confluence, the medium was removed, and the cells were digested with 0.25% trypsin and collected. The cell suspension was centrifugated at 1,000 rpm for 5 min, resuspended in 1 mL of MSC culture medium containing 1% penicillin/streptomycin and 5% FBS, and then cultured in a 10-cm culture dish under the condition of 37°C, 5% CO_2 (1:4 inoculum). The medium was changed every 3 days.

3T3 cells (CRL1658, ATCC) were kindly provided by the Kunming Cell Bank, Chinese Academy of Sciences (Kunming, China). 3T3 cells were cultured in DMEM supplemented with 10% FBS, 100 U/mL penicillin, and 100 μg/mL streptomycin, and glutamine at 37°C in a humidified atmosphere consisting of 5% CO_2. Following the medium change, cells began to proliferate rapidly, and when cells reached 70%–80% confluence, fusion passage culture and cells collection were performed.

Antimicrobial testing

E. coli ATCC25922 was used for the antibacterial studies. A bacterial solution was prepared by adding 3 mL of LB (Luria-Bertani) medium and 300 μL of ampicillin to 10 μL of an *E. coli* solution. The *E. coli* solution was incubated at 37°C at 200 rpm for 24 h. Then, the bacterial solution was employed to study antibacterial effects of the bioinks. Mature biofilms, collected after 1, 3, and 5 days of culture in the presence of a subinhibitory concentration of *E. coli* (Gram negative) or fungi were resuspended in 0.9% normal saline. The biofilms were stained in a dark chamber for 10 min at room temperature with Syto9 (Thermo Fisher Scientific, Waltham,

Please cite this article in press as: Liu et al., Intrinsically cryopreservable, bacteriostatic, durable glycerohydrogel inks for 3D bioprinting, Matter (2023), https://doi.org/10.1016/j.matt.2022.12.013

MA, USA) and propidium iodide (PI) (Sigma-Aldrich, St. Louis, MO, USA) at final concentrations of 2 nmol/mL and 20 nmol/mL, respectively. Ten microliters of staining solution was pipetted onto the biofilms, and the slides were immediately covered with a coverslip. All specimens were examined under a laser confocal microscopic system (TCS SP8, Leica, Germany).

The monoclonal colony *E. coli* solution was cultured at 37°C with shaking at 200 rpm, and the absorbance value was recorded at optical density 600 (OD_{600}) each day.

SEM

Mature biofilms incubated with *E. coli* (Gram negative) bacteria or fungi were collected, placed onto slides, and fixed with 2.5% glutaraldehyde for 5 h at ~ 4°C. After gently washing 3 times with 0.1 mol/L phosphate buffer, the samples were dehydrated using a graded series of alcohol steps and then isoamyl acetate and finally subjected to critical point drying with liquid carbon dioxide to protect the integrity of the biofilm. After metal spraying, a Hitachi SU8000 scanning electron microscope was used to observe and take pictures.

3D laser surface scanning

A 3D laser scanning system was used for the shape analysis. The surface image data were collected from the positive mold and the scaffolds using a Konica Minolta Vivid 910 and Polygen Editing Tools v.2.21 (Konica Minolta, Tokyo, Japan). These data were further processed by Rapid Form 2006 (INUS, Seoul, South Korea) and HP xw6200 (Hewlett Packard, Shanghai, China). The data obtained from the scaffolds were compared with those from the positive mold, which served as a standard. Variations in voxels smaller than 1 mm were considered similar, and the number of these similar voxels was divided by the number of total voxels to calculate the similarity level.

Cytocompatibility

Cell viability was determined by staining viable cells with the green fluorescent dye Calcein AM and necrotic cells with the red fluorescent dye PI (Calcein/PI Cell Viability/Cytotoxicity Assay Kit, Beyotime, China) following the manufacturer's instructions. Images were recorded using a fluorescence microscope (DMI3000B, Leica, Germany).

The CCK-8 assay (Do Jindo Laboratories, Japan) was performed to determine cell viability according to the manufacturer's instructions. In brief, 1×10^4 cells were seeded in each well of a 96-well plate and washed three times with serum-free medium. CCK-8 working buffer (200 μL) was added to each well and incubated in a cell incubator for 2 h. A microplate reader (Thermo Fisher Scientific) was used to detect the absorbance at OD_{450} , and the absorbance value was recorded at OD_{450} each day.

3D bioprinting

Glycerohydrogels were put in a water bath (90°C) for 12 h to melt completely. After cooling to 37°C, the glycerohydrogel was mixed uniformly with cell seed solution at a volume ratio of 20:1. The solution was then placed in the refrigerator for use. The printing was carried out using a 3D printer (BS4.2, Gesim, Germany) with a micronozzle of 220 μm inner diameter, printing speed of 1.2 mm/s, and air pressure of 115 kPa under ambient conditions. All 3D models were designed using 3D Builder or Gesim Robotics software. For bioprinting, glycerohydrogel ink containing 3T3 cells or ADSCs (1×10^6/mL) were used without support bath material. The viabilities of the cells enclosed in the glycerohydrogel obtained through the printing process were determined by staining the cells with the fluorescent dyes Calcein-AM and PI.

Please cite this article in press as: Liu et al., Intrinsically cryopreservable, bacteriostatic, durable glycerohydrogel inks for 3D bioprinting, Matter (2023), https://doi.org/10.1016/j.matt.2022.12.013

Cryopreserved cell viability assay

For cryopreservation, glycerohydrogel ink containing 3T3 cells or ADSCs (1×10^6/mL) were cryopreserved at −80°C and liquid nitrogen (−196°C) without cryoprotectant. Cryopreserved cell viability was determined by staining viable cells with the green fluorescent dye Calcein AM and necrotic cells with the red fluorescent dye PI following the manufacturer's instructions. All specimens were examined under a laser confocal microscopic system (TCS SP8, Leica, Germany).

Statistical analysis

Comparisons between groups were made using Student's t test. Values of $p < 0.05$ were considered to indicate significance. All quantitate data were presented as mean ± standard deviation.

SUPPLEMENTAL INFORMATION

Supplemental information can be found online at https://doi.org/10.1016/j.matt.2022.12.013.

ACKNOWLEDGMENTS

This work was supported by the National Key Research and Development Program of China (2021YFC2400802 and 2021YFC2101800), the National Natural Science Foundation of China (52173117, 21991123, and 82070430), the Ningbo 2025 Science and Technology Major Project (2019B10068), the Natural Science Foundation of Shanghai (20ZR1402500 and 20ZR1434500), the Belt & Road Young Scientist Exchanges Project of Science and Technology Commission Foundation of Shanghai (20520741000), the Science and Technology Commission of Shanghai Municipality (20DZ2254900 and 20DZ2270800), the Biomedical Engineering Fund of Shanghai Jiao Tong University (YG2021GD04), and the Science and Technology Development Foundation of Shanghai Pudong (PKJ2020-Y06).

AUTHOR CONTRIBUTIONS

Conceptualization, M.L., S.J., W.F., and Z.Y.; methodology, M.L., S.J., and H.W.; validation, M.L. and S.J.; formal analysis, M.L. and S.J.; investigation, M.L. and S.J.; resources, W.W., W.F., and Z.Y.; writing – original draft, M.L. and S.J.; writing – review & editing, N.W., W.W., W.F., and Z.Y.; visualization, M.L. and S.J.; supervision, W.W., W.F., and Z.Y.; project administration, W.F. and Z.Y.

DECLARATION OF INTERESTS

The authors declare no competing interests.

Received: September 7, 2022
Revised: November 30, 2022
Accepted: December 21, 2022
Published: February 14, 2023

REFERENCES

1. Lee, A., Hudson, A.R., Shiwarski, D.J., Tashman, J.W., Hinton, T.J., Yerneni, S., Bliley, J.M., Campbell, P.G., and Feinberg, A.W. (2019). 3D bioprinting of collagen to rebuild components of the human heart. Science *365*, 482–487.

2. Grigoryan, B., Paulsen, S.J., Corbett, D.C., Sazer, D.W., Fortin, C.L., Zaita, A.J., Greenfield, P.T., Calafat, N.J., Gounley, J.P., Ta, A.H., et al. (2019). Multivascular networks and functional intravascular topologies within biocompatible hydrogels. Science *364*, 458–464.

3. Jorgensen, A.M., Yoo, J.J., and Atala, A. (2020). Solid organ bioprinting: strategies to achieve organ function. Chem. Rev. *120*, 11093–11127.

4. van der Elst, L., Faccini de Lima, C., Gokce Kurtoglu, M., Koraganji, V.N., Zheng, M., and Gumennik, A. (2021). 3D printing in fiber-device technology. Adv. Fiber Mater. *3*, 59–75.

5. Zou, S., Fan, S., Oliveira, A.L., Yao, X., Zhang, Y., and Shao, H. (2022). 3D printed gelatin scaffold with improved shape fidelity and cytocompatibility by using Antheraea pernyi

Please cite this article in press as: Liu et al., Intrinsically cryopreservable, bacteriostatic, durable glycerohydrogel inks for 3D bioprinting, Matter (2023), https://doi.org/10.1016/j.matt.2022.12.013

silk fibroin nanofibers. Adv. Fiber Mater. *4*, 758–773.

6. Urciuolo, A., Poli, I., Brandolino, L., Raffa, P., Scattolini, V., Laterza, C., Giobbe, G.G., Zambaiti, E., Selmin, G., Magnussen, M., et al. (2020). Intravital three-dimensional bioprinting. Nat. Biomed. Eng. *4*, 901–915.

7. Jian, Y., Handschuh-Wang, S., Zhang, J., Lu, W., Zhou, X., and Chen, T. (2021). Biomimetic anti-freezing polymeric hydrogels: keeping soft-wet materials active in cold environments. Mater. Horiz. *8*, 351–369.

8. Ju, X., Liu, X., Zhang, Y., Chen, X., Chen, M., Shen, H., Feng, Y., Liu, J., Wang, M., and Shi, Q. (2022). A photo-crosslinked proteinogenic hydrogel enabling self-recruitment of endogenous TGF-β1 for cartilage regeneration. Smart Mater. Med. *3*, 85–93.

9. Leng, F., Zheng, M., and Xu, C. (2021). 3D-printed microneedles with open groove channels for liquid extraction. Exploration *1*, 20210109.

10. Li, C., Faulkner-Jones, A., Dun, A.R., Jin, J., Chen, P., Xing, Y., Yang, Z., Li, Z., Shu, W., Liu, D., and Duncan, R.R. (2015). Rapid formation of a supramolecular polypeptide-DNA hydrogel for in situ three-dimensional multilayer bioprinting. Angew. Chem. Int. Ed. Engl. *54*, 3957–3961.

11. Mihara, H., Kugawa, M., Sayo, K., Tao, F., Shinohara, M., Nishikawa, M., Sakai, Y., Akama, T., and Kojima, N. (2019). Improved oxygen supply to multicellular spheroids using A gas-permeable plate and embedded hydrogel beads. Cells *8*, 525.

12. Gao, F., Xu, Z., Liang, Q., Li, H., Peng, L., Wu, M., Zhao, X., Cui, X., Ruan, C., and Liu, W. (2019). Osteochondral regeneration with 3D-printed biodegradable high-strength supramolecular polymer reinforced-gelatin hydrogel scaffolds. Adv. Sci. *6*, 1900867.

13. Zhang, J., Zeng, L., Qiao, Z., Wang, J., Jiang, X., Zhang, Y.S., and Yang, H. (2020). Functionalizing double-network hydrogels for applications in remote actuation and in low-temperature strain sensing. ACS Appl. Mater. Interfaces *12*, 30247–30258.

14. Zhang, C., Zhou, Y., Zhang, L., Wu, L., Chen, Y., Xie, D., and Chen, W. (2018). Hydrogel cryopreservation system: an effective method for cell storage. Int. J. Mol. Sci. *19*, 3330.

15. Cagol, N., Bonani, W., Maniglio, D., Migliaresi, C., and Motta, A. (2018). Effect of cryopreservation on cell-laden hydrogels: comparison of different cryoprotectants. Tissue Eng. Part C Methods *24*, 20–31.

16. Luo, Z., Tang, G., Ravanbakhsh, H., Li, W., Wang, M., Kuang, X., Garciamendez-Mijares, C.E., Lian, L., Yi, S., Liao, J., et al. (2022). Vertical extrusion cryo(bio)printing for anisotropic tissue manufacturing. Adv. Mater. *34*, e2108931.

17. Ravanbakhsh, H., Luo, Z., Zhang, X., Maharjan, S., Mirkarimi, H.S., Tang, G., Chávez-Madero, C., Mongeau, L., and Zhang, Y.S. (2022). Freeform cell-laden cryobioprinting for shelf-ready tissue fabrication and storage. Matter *5*, 573–593.

18. Chrisnandy, A., Blondel, D., Rezakhani, S., Broguiere, N., and Lutolf, M.P. (2022). Synthetic dynamic hydrogels promote degradation-independent in vitro organogenesis. Nat. Mater. *21*, 479–487.

19. Griffin, D.R., Archang, M.M., Kuan, C.H., Weaver, W.M., Weinstein, J.S., Feng, A.C., Ruccia, A., Sideris, E., Ragkousis, V., Koh, J., et al. (2021). Activating an adaptive immune response from a hydrogel scaffold imparts regenerative wound healing. Nat. Mater. *20*, 560–569.

20. Fichman, G., Andrews, C., Patel, N.L., and Schneider, J.P. (2021). Antibacterial gel coatings inspired by the cryptic function of a mussel byssal peptide. Adv. Mater. *33*, e2103677.

21. Murphy, R., Kordbacheh, S., Skoulas, D., Ng, S., Suthiwanich, K., Kasko, A.M., Cryan, S.A., Fitzgerald-Hughes, D., Khademhosseini, A., Sheikhi, A., and Heise, A. (2021). Three-dimensionally printable shear-thinning triblock copolypeptide hydrogels with antimicrobial potency. Biomater. Sci. *9*, 5144–5149.

22. Sani, E.S., Lara, R.P., Aldawood, Z., Bassir, S.H., Nguyen, D., Kantarci, A., Intini, G., and Annabi, N. (2019). An antimicrobial dental light curable bioadhesive hydrogel for treatment of peri-implant diseases. Matter *1*, 926–944.

23. Eelkema, R., and Pich, A. (2020). Pros and cons: supramolecular or macromolecular: what is best for functional hydrogels with advanced properties? Adv. Mater. *32*, e1906012.

24. Zhang, D., Liu, Y., Liu, Y., Peng, Y., Tang, Y., Xiong, L., Gong, X., and Zheng, J. (2021). A general crosslinker strategy to realize intrinsic frozen resistance of hydrogels. Adv. Mater. *33*, e2104006.

25. Gun'ko, V.M., Savina, I.N., and Mikhalovsky, S.V. (2017). Properties of water bound in hydrogels. Gels *3*, 37.

26. Surowiec, R.K., Allen, M.R., and Wallace, J.M. (2022). Bone hydration: how we can evaluate it, what can it tell us, and is it an effective therapeutic target? Bone Rep. *16*, 101161.

27. Youssef, R., Hafez, V., Elkholy, Y., and Mourad, A. (2021). Glycerol 85% efficacy on atopic skin and its microbiome: a randomized controlled trial with clinical and bacteriological evaluation. J. Dermatolog. Treat. *32*, 730–736.

28. Highley, C.B., Rodell, C.B., and Burdick, J.A. (2015). Direct 3D printing of shear-thinning hydrogels into self-healing hydrogels. Adv. Mater. *27*, 5075–5079.

29. Pereira, R.F., Sousa, A., Barrias, C.C., Bártolo, P.J., and Granja, P.L. (2018). A single-component hydrogel bioink for bioprinting of bioengineered 3D constructs for dermal tissue engineering. Mater. Horiz. *5*, 1100–1111.

30. Bertlein, S., Brown, G., Lim, K.S., Jungst, T., Boeck, T., Blunk, T., Tessmar, J., Hooper, G.J., Woodfield, T.B.F., and Groll, J. (2017). Thiol-ene clickable gelatin: a platform bioink for multiple 3D biofabrication technologies. Adv. Mater. *29*, 1703404.

31. Cai, G., Wang, J., Qian, K., Chen, J., Li, S., and Lee, P.S. (2017). Extremely stretchable strain sensors based on conductive self-healing dynamic cross-links hydrogels for human-motion detection. Adv. Sci. *4*, 1600190.

32. Bigi, A., Cojazzi, G., Panzavolta, S., Rubini, K., and Roveri, N. (2001). Mechanical and thermal properties of gelatin films at different degrees of glutaraldehyde crosslinking. Biomaterials *22*, 763–768.

33. Hull, S.M., Brunel, L.G., and Heilshorn, S.C. (2022). 3D bioprinting of cell-laden hydrogels for improved biological functionality. Adv. Mater. *34*, e2103691.

34. He, Q., Huang, Y., and Wang, S. (2018). Hofmeister effect-assisted one step fabrication of ductile and strong gelatin hydrogels. Adv. Funct. Mater. *28*, 1705069.

35. Qin, Z., Sun, X., Zhang, H., Yu, Q., Wang, X., He, S., Yao, F., and Li, J. (2020). A transparent, ultrastretchable and fully recyclable gelatin organohydrogel based electronic sensor with broad operating temperature. J. Mater. Chem. *8*, 4447–4456.

36. Chen, X., Yang, T., Kataoka, S., and Cremer, P.S. (2007). Specific ion effects on interfacial water structure near macromolecules. J. Am. Chem. Soc. *129*, 12272–12279.

37. Chandler, D. (2005). Interfaces and the driving force of hydrophobic assembly. Nature *437*, 640–647.

38. Lee, S.C., Gillispie, G., Prim, P., and Lee, S.J. (2020). Physical and chemical factors influencing the printability of hydrogel-based extrusion bioinks. Chem. Rev. *120*, 10834–10886.

39. Rastin, H., Ormsby, R.T., Atkins, G.J., and Losic, D. (2020). 3D bioprinting of methylcellulose/gelatin-methacryloyl (MC/GelMA) bioink with high shape integrity. ACS Appl. Bio Mater. *3*, 1815–1826.

40. Rutz, A.L., Hyland, K.E., Jakus, A.E., Burghardt, W.R., and Shah, R.N. (2015). A multimaterial bioink method for 3D printing tunable, cell-compatible hydrogels. Adv. Mater. *27*, 1607–1614.

41. Jeon, O., Bin Lee, Y., Hinton, T.J., Feinberg, A.W., and Alsberg, E. (2019). Cryopreserved cell-laden alginate microgel bioink for 3D bioprinting of living tissues. Mater. Today Chem. *12*, 61–70.

42. He, Z., and Yuan, W. (2021). Adhesive, stretchable, and transparent organohydrogels for antifreezing, antidrying, and sensitive ionic skins. ACS Appl. Mater. Interfaces *13*, 1474–1485.

43. Chen, F., Zhou, D., Wang, J., Li, T., Zhou, X., Gan, T., Handschuh-Wang, S., and Zhou, X. (2018). Rational fabrication of anti-freezing, non-drying tough organohydrogels by one-pot solvent displacement. Angew. Chem. Int. Ed. Engl. *57*, 6568–6571.

44. Zeng, L., He, J., Cao, Y., Wang, J., Qiao, Z., Jiang, X., Hou, L., and Zhang, J. (2021). Tissue-adhesive and highly mechanical double-network hydrogel for cryopreservation and sustained release of anti-cancer drugs. Smart Mater. Med. *2*, 229–236.

45. Sun, L., Chen, S., Guo, Y., Song, J., Zhang, L., Xiao, L., Guan, Q., and You, Z. (2019). Ionogel-based, highly stretchable, transparent, durable

Please cite this article in press as: Liu et al., Intrinsically cryopreservable, bacteriostatic, durable glycerohydrogel inks for 3D bioprinting, Matter (2023), https://doi.org/10.1016/j.matt.2022.12.013

triboelectric nanogenerators for energy harvesting and motion sensing over a wide temperature range. Nano Energy *63*, 103847.

46. Sun, L., Huang, H., Ding, Q., Guo, Y., Sun, W., Wu, Z., Qin, M., Guan, Q., and You, Z. (2022). Highly transparent, stretchable, and self-healable ionogel for multifunctional sensors, triboelectric nanogenerator, and wearable fibrous electronics. Adv. Fiber Mater. *4*, 98–107.

47. Sun, L., Huang, H., Guan, Q., Yang, L., Zhang, L., Hu, B., Neisiany, R.E., You, Z., and Zhu, M. (2022). Cooperative chemical coupling and physical lubrication effects construct highly dynamic ionic covalent adaptable network for high-performance wearable electronics. CCS Chem, 1–12. https://doi.org/10.31635/ccschem.022.20220203.

48. Song, J., Chen, S., Sun, L., Guo, Y., Zhang, L., Wang, S., Xuan, H., Guan, Q., and You, Z. (2020). Mechanically and electronically robust transparent organohydrogel fibers. Adv. Mater. *32*, e1906994.

49. Cerveny, S., Colmenero, J., and Alegría, A. (2005). Dielectric investigation of the low-temperature water dynamics in the poly(vinyl methyl ether)/H2O system. Macromolecules *38*, 7056–7063.

50. Hook, A.L., Chang, C.Y., Yang, J., Luckett, J., Cockayne, A., Atkinson, S., Mei, Y., Bayston, R., Irvine, D.J., Langer, R., et al. (2012). Combinatorial discovery of polymers resistant to bacterial attachment. Nat. Biotechnol. *30*, 868–875.

51. Le Thi, P., Lee, Y., Hoang Thi, T.T., Park, K.M., and Park, K.D. (2018). Catechol-rich gelatin hydrogels in situ hybridizations with silver nanoparticle for enhanced antibacterial activity. Mater. Sci. Eng. C Mater. Biol. Appl. *92*, 52–60.

52. Zhang, H., Ma, J., Liu, C., Li, L., Xu, C., Li, Y., Li, Y., and Tian, H. (2022). Antibacterial activity of guanidinium-based ionic covalent organic framework anchoring Ag nanoparticles. J. Hazard Mater. *435*, 128965.

53. Thajai, N., Jantanasakulwong, K., Rachtanapun, P., Jantrawut, P., Kiattipornpithak, K., Kanthiya, T., and Punyodom, W. (2022). Effect of chlorhexidine gluconate on mechanical and anti-microbial properties of thermoplastic cassava starch. Carbohydr. Polym. *275*, 118690.

54. Saegeman, V.S.M., Ectors, N.L., Lismont, D., Verduyckt, B., and Verhaegen, J. (2008). Short- and long-term bacterial inhibiting effect of high concentrations of glycerol used in the preservation of skin allografts. Burns *34*, 205–211.

55. Gjorevski, N., Nikolaev, M., Brown, T.E., Mitrofanova, O., Brandenberg, N., DelRio, F.W., Yavitt, F.M., Liberali, P., Anseth, K.S., and Lutolf, M.P. (2022). Tissue geometry drives deterministic organoid patterning. Science *375*, eaaw9021.

56. Gillispie, G., Prim, P., Copus, J., Fisher, J., Mikos, A.G., Yoo, J.J., Atala, A., and Lee, S.J. (2020). Assessment methodologies for extrusion-based bioink printability. Biofabrication *12*, 022003.

57. Lewis, D.A., Young, P.M., Buttini, F., Church, T., Colombo, P., Forbes, B., Haghi, M., Johnson, R., O'Shea, H., Salama, R., and Traini, D. (2014). Towards the bioequivalence of pressurised metered dose inhalers 1: design and characterisation of aerodynamically equivalent beclomethasone dipropionate inhalers with and without glycerol as a non-volatile excipient. Eur. J. Pharm. Biopharm. *86*, 31–37.

58. Terakosolphan, W., Trick, J.L., Royall, P.G., Rogers, S.E., Lamberti, O., Lorenz, C.D., Forbes, B., and Harvey, R.D. (2018). Glycerol solvates DPPC headgroups and localizes in the interfacial regions of model pulmonary interfaces altering bilayer structure. Langmuir *34*, 6941–6954.

59. Murray, K.A., and Gibson, M.I. (2022). Chemical approaches to cryopreservation. Nat. Rev. Chem *6*, 579–593.

60. Terakosolphan, W., Altharawi, A., Poonprasartporn, A., Harvey, R.D., Forbes, B., and Chan, K.L.A. (2021). In vitro Fourier transform infrared spectroscopic study of the effect of glycerol on the uptake of beclomethasone dipropionate in living respiratory cells. Int. J. Pharm. *609*, 121118.

61. Janati Idrissi, S., Le Bourhis, D., Lefevre, A., Emond, P., Le Berre, L., Desnoës, O., Joly, T., Buff, S., Freret, S., Schibler, L., et al. (2022). Effects of the donor factors and freezing protocols on the bovine embryonic lipid profile. Biol. Reprod. *106*, 597–612.

62. Yin, S., Su, G., Chen, J., Peng, X., and Zhou, T. (2021). Ultra-Stretchable and self-healing anti-freezing strain sensors based on hydrophobic associated polyacrylic acid hydrogels. Materials *14*, 6165.

63. Ma, Y., Gao, L., Tian, Y., Chen, P., Yang, J., and Zhang, L. (2021). Advanced biomaterials in cell preservation: hypothermic preservation and cryopreservation. Acta Biomater. *131*, 97–116.